Extremophiles (2009) 13:481–489
DOI 10.1007/s00792-009-0233-7

ORIGINAL PAPER

The contribution of proline residues to protein stability is associated with isomerization equilibrium in both unfolded and folded states

Meng Ge · Xian-Ming Pan

Received: 1 November 2008 / Accepted: 11 February 2009 / Published online: 5 March 2009

Abstract It has long been understood that the proline residue has lower configurational entropy than any other amino acid residue due to pyrrolidine ring hindrance. The peptide bond between proline and its preceding amino acid (Xaa-Pro) typically exists as a mixture of *cis*- and *trans*-isomers in the unfolded protein. *Cis–trans* isomerization of Xaa-Pro peptide bonds are infrequent, but still occur in folded proteins. Therefore, the effects of the *cis–trans* isomerization equilibrium in both unfolded and folded states should be taken into account when estimating the stability contribution of a specific proline residue. In order to study the stability contribution of the four proline residues to the hyperthermophilic protein Ssh10b, in this work, we expressed and purified a series of Pro→Ala mutants of Ssh10b, and performed correlative unfolding experiments in detail. We proposed a new unfolding model including proline isomerization. The model predicts that the contribution of a proline residue to protein stability is associated with the thermodynamic equilibrium between *cis*- and *trans*-isomers both in the unfolded and folded states, agreeing well with the experimental results.

Keywords Protein stability · *Cis–trans* isomerization · Circular dichroism · Unfolding

Communicated by A. Driessen.

M. Ge · X.-M. Pan (✉)
The Key Laboratory of Bioinformatics, Ministry of Education, Department of Biological Sciences and Biotechnology, Tsinghua University, 100084 Beijing, China
e-mail: pan-xm@mail.tsinghua.edu.cn

Introduction

It has long been understood that the proline residue has lower configurational entropy than any other amino acid residue in the unfolded form due to pyrrolidine ring hindrance (Matthews et al. 1987; Suzuki et al. 1987; Suzuki 1989). Since Matthews et al. showed in 1987 that the thermostability of bacteriophage T4 lysozyme could be enhanced by replacing an alanine with a proline, the decreasing entropy theory has been verified by many reports: replacing Xaa (representing any other amino acid) with Pro has resulted in enhanced thermostability in *Bacillus stearothermophilus* neutral protease (Hardy et al. 1993), *Bacillus cereus* ATCC7064 oligo-1, 6-glucosidase (Watanabe et al. 1994), *Aspergillus awamori* glucoamylase (Li et al. 1997; Allen et al. 1998), *Serratia marcescens* chitinase (Gåseidnes et al. 2003), and *Clostridium beijerinckii* alcohol dehydrogenase (Goihberg et al. 2007). Replacing Pro with Xaa has been reported to decrease thermostability in *Thermotoga neapolitana* xylose isomerase (Sriprapundh et al. 2000), decrosin (Frare et al. 2005), and *Thermus aquaticus* aqualysin I (Sakaguchi et al. 2007).

The peptide bond between proline and its preceding amino acid (Xaa-Pro) in unfolded proteins typically exists as a mixture of *cis*- and *trans*-isomers with a *cis*-content of about 10–30% depending on the primary sequence (Cheng and Bovey 1977; Grathwohl and Wüthrich 1981), implying that the free energy of the *trans*-isomer is about 2–5 kJ/mol lower than that of the *cis*-isomer at room temperature ($\Delta G = -RT \ln(K)$). *Cis–trans* isomerization of the Xaa-Pro peptide bonds are infrequent, but still occur in folded proteins. Therefore, the *cis–trans* isomerization equilibrium in both unfolded and folded states should be taken into account when estimating the stability contribution of a specific proline residue to protein stability.

The DNA binding protein Ssh10b from the archaeon *Sulfolobus shibatae*, a member of the Sac10b family, is conserved in most thermophilic and hyperthermophilic archaeal genomes that have been sequenced to date (Xue et al. 2000). This protein constitutes about 4–5% of cellular protein, and binds dsDNA without apparent sequence specificity. Ssh10b is capable of constraining negative DNA supercoils in a temperature dependent fashion. This ability is weak at 25°C, but is enhanced substantially at temperatures of 45°C and higher. Ssh10b is a highly thermostable dimeric protein composed of two identical subunits (Xu et al. 2004). Each monomer contains 97 amino acid residues, and has four proline residues located at positions 6, 8, 18, and 62. Heteronuclear nuclear magnetic resonance (NMR) and site-directed mutagenesis analysis indicate that two native forms of the Ssh10b homodimer co-exist in solution due to slow *cis–trans* isomerization of the Leu^{61}-Pro^{62} peptide bond (Cui et al. 2003). The T-form dimer, with the Leu^{61}-Pro^{62} peptide bonds of both monomers in the *trans*-conformation, dominates at higher temperatures; while the C-form dimer, with the Leu^{61}-Pro^{62} peptide bonds of both monomers in the *cis*-conformation, dominates at lower temperatures. The two forms of the Ssh10b homodimers have the same DNA binding site but have different conformational features that are responsible for the temperature-dependent nature of the Ssh10b-DNA interaction (Cui et al. 2003).

In the present work, a series of Pro→Ala mutants of Ssh10b (P6A, P8A, P18A, P62A, P18AP62A, and P6AP8AP18AP62A) were constructed by site-directed mutagenesis to study the stability contribution of the four proline residues. Stability of Ssh10b wild-type and its mutants was investigated through unfolding experiments monitored by circular dichroism (CD) in detail. A new unfolding model was proposed in which the *cis–trans* isomerization of the peptide bonds between the proline residue and its preceding residue was taken into account. According to this model, the contribution of a proline residue to protein stability is associated with the thermodynamic equilibrium between the *cis*- and *trans*-isomers in both the unfolded and folded states.

Materials and methods

Materials

HEPES, Urea, Tris, and isopropyl β-D-thiogalactoside (IPTG) were purchased from Sigma. The expression plasmid pET11a-*ssh10b* containing the *ssh10b* gene, and host strains *E. coli* DH5α and BL21 (DE3) were from our laboratory stocks. Enzymes and reagents for DNA manipulations were purchased from Takara. Plasmid miniprep kits were obtained from Qiagen. All chromatography apparatus and materials were purchased from GE Healthcare.

Expression and purification of Ssh10b and its variants

All expression plasmids of Ssh10b variants were constructed from the parental plasmid pET11a-*ssh10b*. All mutations were introduced by site-directed mutagenesis through overlap extension PCR. The construct for each variant was verified by commercial DNA sequencing at Takara Biotechnology (Dalian) Co. Ltd.

Expression plasmids of Ssh10b and its variants were transformed into the *E. coli* BL21 (DE3) host strain. Wild-type Ssh10b and its variants were expressed and purified to homogeneity in the same way as previously described (Xu et al. 2004) except that the UNO S6 column (Biorad) was substituted with a 6 ml Resource S column (GE Healthcare). The protein samples were dialyzed against 50 mM NH_4HCO_3, lyophilized and stored at −20°C.

CD spectra characterization of Ssh10b and its variants

Ssh10b and its variants were characterized by CD spectra, which were recorded in 20 mM Na_2HPO_4-NaH_2PO_4/pH 6.8 with a π*-pistar 180 spectrometer (Applied Photophysics Ltd, UK) by using a rectangular quartz cuvette with a path length of 1 mm. Far-UV CD spectra were recorded from 200 to 250 nm at a protein concentration of 50 μM at 25°C, while near-UV CD spectra were recorded from 250 to 300 nm at a protein concentration of 1 mM at 70°C. Each spectrum was the average of four scans and was corrected for spurious signals generated by the solvent.

Unfolding studies

In this study, the protein concentration used at all unfolding experiments is about 50 μM (monomer concentration). Urea-induced unfolding of Ssh10b and its variants was studied by taking CD measurements, performed in buffer H (10 mM HEPES/pH 7.0). The CD signal was monitored using a rectangular quartz cuvette with a path length of 1 mm. The urea solution was freshly prepared on the day of use. Samples containing various concentrations of urea were equilibrated at 25°C overnight and then measured by far-UV CD at 222 nm.

Heat-induced unfolding of Ssh10b and its variants was also performed in buffer H by measuring far-UV CD at 222 nm. Each sample was heated from 40 to 98°C and then cooled from 98 to 40°C using stepwise changes of 2°C, and the CD signal was recorded after equilibration for 2 min at each temperature point. During the entire experiment CD spectra were recorded before heating, after heating, and

after cooling. Spectra were scanned at 1 nm intervals from 200 to 250 nm.

Analysis of the denaturation data

Previous work of our laboratory has shown that both denaturant- and heat-induced unfolding of Ssh10b are fully reversible, and follow a two-state mechanism involving a native dimer and two denatured monomers (Xu et al. 2004). Therefore, in this work the thermodynamic properties of Ssh10b and its variants were calculated assuming a two-state denaturation process: $N_2 \overset{K_{obs}}{\leftrightarrow} 2U$ (Xu et al. 2004). The observed equilibrium constant (K_{obs}) and the corresponding free energy change (ΔG) at temperature T or denaturant concentration $[D]$ were calculated from the CD data according to:

$$K_{obs} = \frac{2 \times P_t}{y_N + m_N T[D] - y_U + m_U T[D]} \times \frac{[y_N + m_N T[D] - y]^2}{y - y_U + m_U T[D]} \quad (1)$$

$$\Delta G = -RT \ln(K_{obs}) \quad (2)$$

Here, P_t is the total protein concentration in monomer units; R is the gas constant; T is the absolute temperature; y is the experimentally measured signal value at a given temperature (T) or given denaturant concentration ($[D]$); y_N and y_U are the intercepts; and m_N and m_U are the slopes of the native and unfolded baselines respectively.

According to the linear free energy model (Schellman 1987; Chen and Schellman 1989; Agashe and Udgaonkar 1995; Kamal et al. 2002), the changes in free energy (ΔG) that occur on unfolding are expected to vary linearly with the denaturant concentration ($[D]$).

$$\Delta G = \Delta G(H_2O) - m_G[D] \quad (3)$$

Here, $\Delta G(H_2O)$ represents the free energy change of unfolding in the absence of denaturant and m_G is the slope of the transition for the free energy.

The unfolding of a proline residue in a dimeric protein, including the *cis–trans* isomerization in both native and unfolded states, can be represented as Scheme 1.

Scheme 1 Thermodynamic unfolding model of a proline residue in dimer

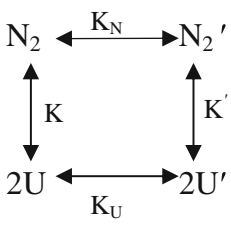

Then,

$$K_N = \frac{[N_2']}{[N_2]} \quad (4)$$

$$K = \frac{[U]^2}{[N_2]} \quad (5)$$

$$K' = \frac{[U']^2}{[N_2']} \quad (6)$$

$$K_U = \frac{[U']}{[U]} \quad (7)$$

Here, $[N_2]$ and $[N_2']$ represent protein concentrations in the *trans*- and *cis*-forms of the native state respectively; $[U]$ and $[U']$ are protein concentrations in the unfolded state in *trans*- and *cis*-forms, respectively; K and K' are the equilibrium constants for unfolding from *trans*- to *trans*-form and from *cis*- to *cis*-form, respectively; and K_N and K_U are the *trans–cis* isomerization equilibrium constants of the native and unfolded states, respectively. Thus the observed equilibrium constant for Pro^{62} unfolding (K_{obs}(P62)) is:

$$K_{obs}(P62) = \frac{([U] + [U'])^2}{[N_2] + [N_2']} = \frac{(1 + K_U(P62))^2}{(1 + K_N(P62))} \times \frac{[U]^2}{[N_2]} = \frac{(1 + K_U(P62))^2}{(1 + K_N(P62))} \times K(P62) \quad (8)$$

Here, K(P62) represents the equilibrium constant of unfolding of Pro^{62} from *trans*- in the native form to *trans*- in the unfolded state. Since there is no evidence for *cis–trans* isomerization at Pro^{18}, the observed equilibrium constant for Pro^{18} unfolding (K_{obs}(P18)) is:

$$K_{obs}(P18) = \frac{([U] + [U'])^2}{[N_2]} = (1 + K_U(P18))^2 \frac{[U]^2}{[N_2]} = (1 + K_U(P18))^2 \times K(P18) \quad (9)$$

Here, K(P18) represents the equilibrium constant of unfolding of Pro^{18} from *trans*- in the native state to *trans*- in the unfolded state.

Furthermore, when proline is replaced by alanine in a homodimer, the apparent equilibrium constant (K^*) of such a substitution can be represented as:

$$K^* = \frac{K(Ala)}{K(Pro)} = \exp\left(-\frac{2\Delta S}{R}\right) \quad (10)$$

Here, ΔS is the configuration entropy difference of a proline residue relative to an alanine residue (Matthews et al. 1987).

For the variant P18AP62A, the observed equilibrium constant (K_{obs}) for unfolding can be represented as:

$$K_{obs}(\text{P18AP62A}) = K(\text{A18}) \times K(\text{A62}) \times K_{rest} \quad (11)$$

Here, K_{rest} represents the equilibrium constant for the unfolding of the protein except for the contribution of the 18th and 62nd residues. Considering the *cis–trans* equilibrium of Pro^{18} and Pro^{62}, the observed equilibrium constant (K_{obs}) for the unfolding of wild-type Ssh10b can be represented as:

$$\begin{aligned} K_{obs}(\text{Wild}) &= K_{obs}(\text{P18}) \times K_{obs}(\text{P62}) \times \text{K}_{rest} \\ &= \frac{(1+K_U(\text{P18}))^2(1+K_U(\text{P62}))^2}{(1+K_N(\text{P62}))} \times K(\text{P18}) \\ &\quad \times K(\text{P62}) \times K_{rest} \end{aligned} \quad (12)$$

Substituting Eqs. 10 and 11 into Eq. 12 gives:

$$\begin{aligned} K_{obs}(\text{Wild}) = &\frac{(1+K_U(\text{P18}))^2(1+K_U(\text{P62}))^2}{(1+K_N(\text{P62})) \times K^*(\text{P18A}) \times K^*(\text{P62A})} \\ &\times K_{obs}(\text{P18AP62A}) \end{aligned} \quad (13)$$

Here, K^*(P18A) and K^*(P62A) are the apparent equilibrium constants for the replacement of Pro^{18} and Pro^{62} with Ala. For the unfolding of P18A, the observed equilibrium constant (K_{obs}(P18A)) can be represented as:

$$\begin{aligned} K_{obs}(\text{P18A}) =& K(\text{A18}) \times K_{obs}(\text{P62}) \times K_{rest} \\ =& \frac{(1+K_U(\text{P62}))^2}{(1+K_N(\text{P62})) \times K^*(\text{P18A})} \\ &\times K_{obs}(\text{P18AP62A}) \end{aligned} \quad (14)$$

For the unfolding of P62A, the observed equilibrium constant (K_{obs}(P62A)) can be represented as:

$$\begin{aligned} K_{obs}(\text{P62A}) &= K_{obs}(\text{P18}) \times K(\text{A62}) \times K_{rest} \\ &= \frac{(1+K_U(\text{P18}))^2}{K^*(\text{P62A})} \times K_{obs}(\text{P18AP62A}) \end{aligned} \quad (15)$$

Assuming that the enthalpy and entropy changes of the *trans–cis* isomerization are temperature independent, then:

$$\begin{aligned} K_N &= \exp\left(-\frac{\Delta G_N}{RT}\right) = \exp\left(-\frac{\Delta H_N - T \times \Delta S_N}{RT}\right) \\ K_U &= \exp\left(-\frac{\Delta G_U}{RT}\right) = \exp\left(-\frac{\Delta H_U - T \times \Delta S_U}{RT}\right) \end{aligned} \quad (16)$$

Here, $\Delta G_N(\Delta G_U)$, $\Delta H_N(\Delta H_U)$, and $\Delta S_N(\Delta S_U)$ represent the free energy, enthalpy, and entropy changes of the *trans–cis* isomerization equilibrium, respectively, in the native (unfolded) state.

For thermal unfolding, assuming that the heat capacity change (ΔC_p) between the native and unfolded states of the system is relatively independent of temperature, then for the mutant P18AP62A (Santoro and Bolen 1988; Freire 1995):

$$\begin{aligned} \Delta G(T) &= -RT\ln(K_{obs}(\text{P18AP62A})) \\ &= \Delta H_m - T\Delta S_m + \Delta C_p \\ &\quad \left((T - T_m) + T\ln\left(1 - \frac{T - T_m}{T}\right)\right) \end{aligned} \quad (17)$$

Here, ΔH_m and ΔS_m are the enthalpy and entropy changes of the mutant, respectively, at the transition midpoint, where $T = T_m$. Within the transition range, where $T\ln\left(1 - \frac{T-T_m}{T}\right) \approx T_m - T$, Eq. 17 can be simplified to the van't Hoff plot:

$$K_{obs}(\text{P18AP62A}) = \exp\left(-\frac{\Delta H_m - T \times \Delta S_m}{RT}\right) \quad (18)$$

Substitution of Eqs. 16 and 18 into Eqs. 13–15, then for the wild-type protein:

$$K_{obs}(\text{Wild}) = \frac{\left(1+\exp\left(-\frac{\Delta H_U(\text{P62}) - T\Delta S_U(\text{P62})}{RT}\right)\right)^2 \left(1+\exp\left(-\frac{\Delta H_U(\text{P18}) - T\Delta S_U(\text{P18})}{RT}\right)\right)^2}{\left(1+\exp\left(-\frac{\Delta H_N(\text{P62}) - T\Delta S_N(\text{P62})}{RT}\right)\right) \times K^*(\text{P18A}) \times K^*(\text{P62A})} \times \exp\left(-\frac{\Delta H_m - T\Delta S_m}{RT}\right) \quad (19)$$

For the variant P18A:

$$\begin{aligned} K_{obs}(\text{P18A}) = &\frac{\left(1+\exp\left(-\frac{\Delta H_U(\text{P62}) - T\Delta S_U(\text{P62})}{RT}\right)\right)^2}{\left(1+\exp\left(-\frac{\Delta H_N(\text{P62}) - T\Delta S_N(\text{P62})}{RT}\right)\right) \times K^*(\text{P18A})} \\ &\times \times \exp\left(-\frac{\Delta H_m - T\Delta S_m}{RT}\right) \end{aligned} \quad (20)$$

For the variant P62A:

$$K_{\mathrm{obs}}(\mathrm{P62A}) = \frac{\left(1+\exp\left(-\frac{\Delta H_{\mathrm{U}}(\mathrm{P18})-T\Delta S_{\mathrm{U}}(\mathrm{P18})}{RT}\right)\right)^2}{K^*(\mathrm{P62A})} \times \exp\left(-\frac{\Delta H_{\mathrm{m}}-T\Delta S_{\mathrm{m}}}{RT}\right) \quad (21)$$

Here, ΔH_{u}(P62), ΔS_{u}(P62), ΔH_{u}(P18), and ΔS_{u}(P18) represent the *trans–cis* isomerization enthalpy and entropy changes of Pro^{62} and Pro^{18}, respectively, in the unfolded state; ΔH_{N}(P62) and ΔS_{N}(P62) represent the *trans–cis* isomerization enthalpy and entropy changes, respectively, of Pro^{62} in the native state; ΔH_{m} and ΔS_{m} represent the unfolding enthalpy and entropy changes, respectively, at the transition midpoint of the variant P18AP62A.

Results

Co-existence of two Ssh10b homodimers with different conformations

Wild-type Ssh10b and its variants were purified to homogeneity in the same way, and the purity of the proteins was confirmed by to be more than 95% by 15% SDS-PAGE. Cation exchange chromatography experiments showed an interesting phenomenon of two adjacent absorbance peaks at UV_{280} in the elution profiles of Ssh10b and the variants without Pro^{62} mutations, while there was only one absorbance peak in the elution profiles of variants with an alanine replacement of Pro^{62}. In order to clarify the molecular basis of this phenomenon, fractions from the two adjacent absorbance peaks of Ssh10b and the absorbance peak of P62A (as shown in Fig. 1) were collected, and analyzed immediately by ultracentrifugation. Our data suggest that the three samples all existed as dimers (data not shown). The two Ssh10b fractions were dialyzed against buffer A (20 mM Na_2HPO_4/NaH_2PO_4, pH 7.5, 1 mM EDTA) overnight, and then applied to the same chromatography column. The two elution profiles were similar to one another and to the original elution profile (Fig. 1). Taken together, these results indicated that there is a kinetic equilibrium between the two forms of Ssh10b in solution due to the presence of Pro^{62}. This is in agreement with published data indicating that two forms of Ssh10b homodimers co-exist in solution because of *cis–trans* isomerization of the Leu^{61}-Pro^{62} peptide bond (Cui et al. 2003).

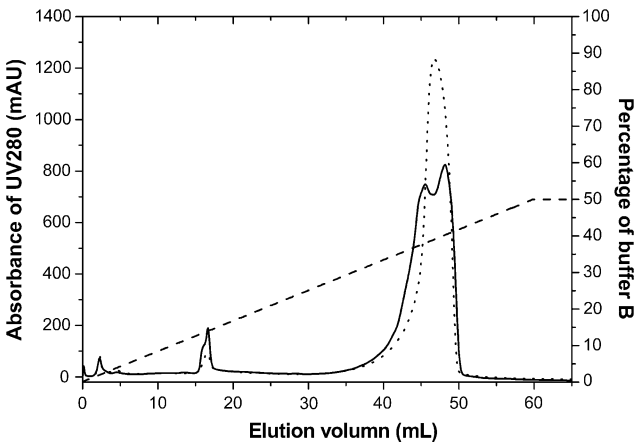

Fig. 1 Elution profiles of wild-type Ssh10b and the P62A variant by cation exchange chromatography: wild-type (*solid line*), P62A (*dotted line*), and percentage of buffer B (*dashed line*)

CD spectra characterization of Ssh10b and its variants

Figure 2a shows that far-UV CD spectra of the Ssh10b wild-type and its variants are almost superimposable, indicating that Pro→Ala replacements do not influence secondary structure. Near-UV CD spectra of the Ssh10b wild-type and its variants are also almost superimposable (Fig. 2b), suggesting that Pro→Ala replacements have no influence on the tertiary structure of the protein.

Unfolding studies

Ssh10b is resistant to urea-induced denaturation in phosphate buffer (Xu et al. 2004), but its stability toward urea-induced denaturation decreases greatly in some monovalent ion buffers (Mao et al. 2007). Figure 3a shows representative urea-induced unfolding profiles for Ssh10b and its variants in buffer H. These proteins can be divided into three groups: high stability (P6A, P8A, and wild-type Ssh10b); intermediate stability (P18A and P62A); and low stability groups (P18AP62A and P6AP8AP18AP62A). The unfolding curves of the proteins from high stability and low stability groups are almost superimposable within each group, while in the intermediate stability group, P18A seems obviously more stable than P62A. The linear free energy model (Schellman 1987; Chen and Schellman 1989; Agashe and Udgaonkar 1995; Kamal et al. 2002) was used to estimate the unfolding free energy of Ssh10b and its variants. The obtained unfolding free energy values were: $\Delta G_{(\text{wild-type})}$ = 55.2 ± 0.6 kJ/mol, $\Delta G_{(\mathrm{P18A})}$ = 47.9 ± 0.7 kJ/mol, $\Delta G_{(\mathrm{P62A})}$ = 44.6 ± 0.5 kJ/mol, and $\Delta G_{(\mathrm{P18AP62A})}$ = 38.4 ± 0.4 kJ/mol. The unfolding free energy values of the three variants (P18A, P62A, and P18AP62A) relative to the native protein decreased by 7.3, 10.6, and 16.8 kJ/mol, respectively. These data suggest that destabilization by the Pro→Ala replacement is roughly additive.

Ssh10b is thermally stable up to 85°C in phosphate buffer (Xu et al. 2004), but we found that its thermostability decreased greatly in HEPES buffer. The heat-induced

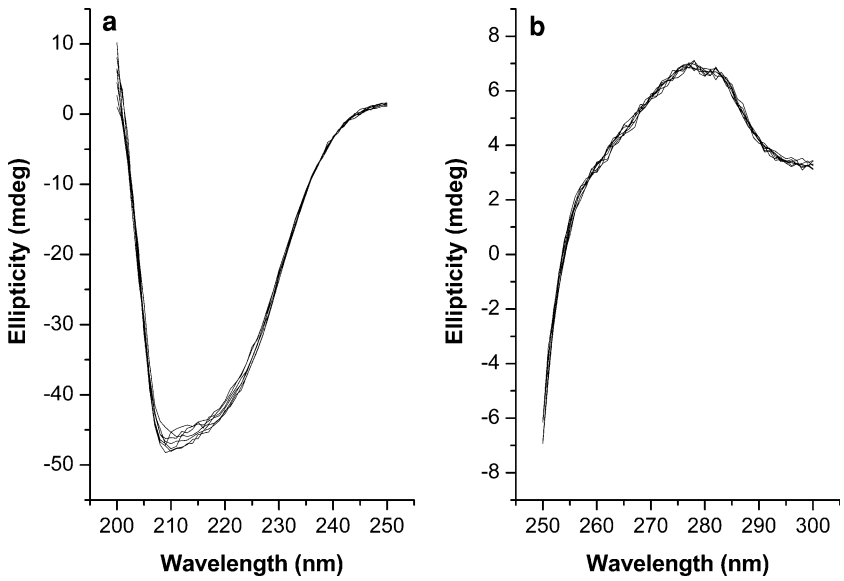

Fig. 2 CD spectra of Ssh10b and its variants: **a** the *seven lines* represent the far-UV spectra of Ssh10b and its variants; **b** the *seven lines* represent the near-UV spectra of Ssh10b and its variants

unfolding and refolding curves of Ssh10b and its variants in buffer H monitored by far-UV CD at 222 nm are nearly superimposable, and for each one the CD spectrum of the refolded protein is nearly identical to that of the native protein (data not shown), indicating that the processes of heat-induced unfolding of Ssh10b and its variants are fully reversible.

Protein stability toward heat-induced unfolding displayed a similar tendency as shown for urea-induced unfolding: heat-induced unfolding profiles of proteins of high stability and low stability groups are almost superimposable within their groups. But for the intermediate stability group, an interesting phenomenon was found: P62A seems slightly more stable than P18A, in contrast to results of urea-induced unfolding. Figure 3b shows the heat-induced unfolding profiles of wild-type Ssh10b, P18A, P62A, and P18AP62A in buffer H. The profiles of P6A and P8A were almost superimposable with that of wild-type Ssh10b, and the profile of P6AP8AP18AP62A was almost superimposable with that of P18AP62A (data not shown).

Heat-induced unfolding profiles were analyzed using the model described in "Materials and methods". The parameters ΔH_N(P62) and ΔS_N(P62) were obtained by fitting the population ratio data of the *cis*-form/*trans*-form Ssh10b homodimer versus temperature from the previous report of Cui et al. (Cui et al. 2003) to Eq. 16. A Pro→Ala replacement was calculated to contribute 4 cal/mol per K to the entropy of denaturation (Némethy et al. 1966; Matthews et al. 1987), therefore K^*(P18A) and K^*(P62A) were obtained by substituting this value into Eq. 10. The parameters ΔH_m and ΔS_m were obtained by fitting K_{obs}(P18AP62A) to Eq. 18. These values were then substituted into the corresponding equations as follows: ΔH_u(P18) and ΔS_u(P18) were obtained by fitting K_{obs}(P62A) to Eq. 21; ΔH_u(P62) and ΔS_u(P62) were obtained by fitting K_{obs}(P18A) to Eq. 20. The values obtained for all these parameters are presented in Table 1. All parameters were substituted into Eq. 19 to reconstruct the wild-type protein unfolding curve. As shown in Fig. 3b, the theoretical unfolding curves of Ssh10b and its variants matched the experimental data perfectly, indicating that these Pro→Ala replacements are independent.

ΔC_p of P18AP62A was obtained by substituting the value of $\Delta G_{(P18AP62A)}$ obtained from urea-induced unfolding experiments at 298 K into Eq. 17. Using Eq. 17, we can deduce $\Delta G_{(P18AP62A)}$ at any specified temperature. The unfolding free energy of P18A, P62A and wild-type Ssh10b at any specified temperature can also be deduced from Eqs. 2, and 13–16. For example, the obtained unfolding free energy values of P18A, P62A and wild-type Ssh10b at 298 K were: $\Delta G_{(wild\text{-}type)}$ = 57.2 ± 0.6 kJ/mol, $\Delta G_{(P18A)}$ = 49.1 ± 0.5 kJ/mol, $\Delta G_{(P62A)}$ = 46.4 ± 0.5 kJ/mol, agreeing well with those obtained from urea-induced unfolding experiments. Figure 4 shows the profiles of the unfolding free energy (ΔG) of these four proteins (wild-type Ssh10b, P18A, P62A, and P18AP62A) versus temperature. As shown in Fig. 4, ΔG for P18A was greater at lower temperatures than ΔG for P62A, but was lower at higher temperatures than that of P62A, in good agreement with experimental results: in the urea-induced unfolding experiment (298 K) P18A was more stable than P62A, while in the heat-induced unfolding experiment P62A was slightly more stable than P18A within the melting region (about 335–360 K).

Discussion

The proline residue has less configurational entropy than any other amino acid residue in the unfolded form due to

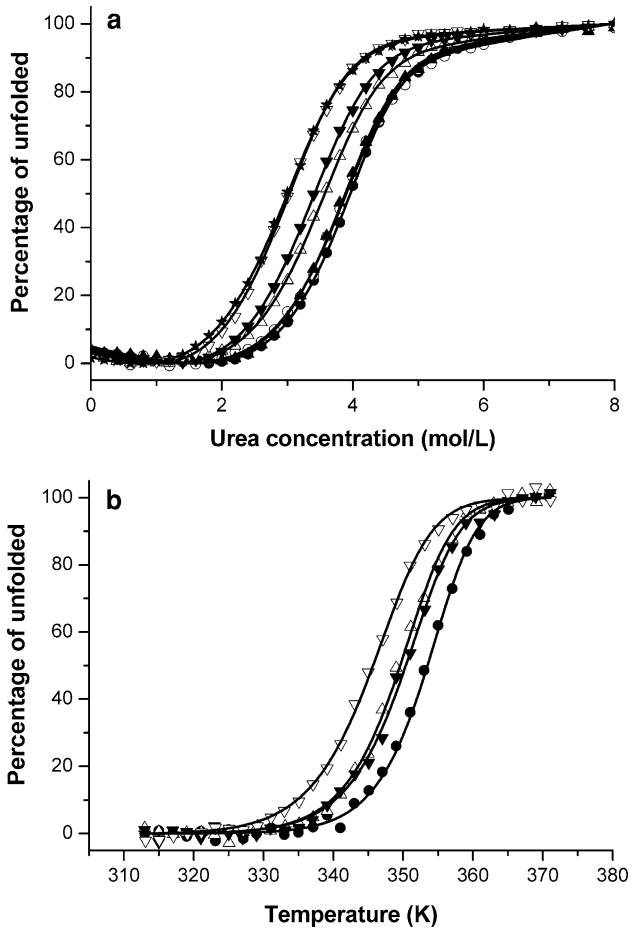

Fig. 3 Unfolding profiles for wild-type Ssh10b and its variants: **a** representative urea-induced unfolding profiles for wild-type Ssh10b (*filled circles*) and its variants: P6A (*open circles*), P8A (*filled triangles*), P18A (*open triangles*), P62A (*filled inverted triangles*), P18AP62A (*open inverted triangles*), and P6AP8AP18AP62A (*filled stars*); *continuous lines* represent the fit of the experimental data to the linear extrapolation model; **b**, representative heat-induced unfolding profiles for wild-type Ssh10b (*filled circles*) and its variants: P18A (*open triangles*), P62A (*filled inverted triangles*), and P18AP62A (*open inverted triangles*); *continuous lines* represent theoretical curves obtained by using the new model

Table 1 Parameters obtained from heat-induced unfolding experiments

Parameter	Value
K^*	56.0
ΔS_m (J/mol per deg)	879.8 ± 18.7
ΔH_m (kJ/mol)	332.6 ± 6.5
T_m (K)	345.7 ± 0.2
ΔC_p (kJ/mol)	9.3 ± 0.2
ΔS_N(P62) (J/mol per deg)	−211.9 ± 5.2
ΔH_N(P62) (kJ/mol)	−65.2 ± 2.1
ΔS_U(P18) (J/mol per deg)	85.0 ± 2.6
ΔH_U(P18) (kJ/mol)	27.2 ± 0.8
ΔS_U(P62) (J/mol per deg)	91.2 ± 2.9
ΔH_U(P62) (kJ/mol)	28.7 ± 1.1

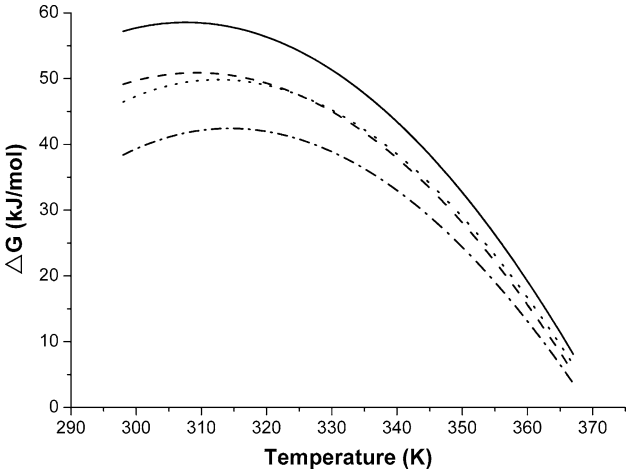

Fig. 4 The profiles of the theoretical unfolding free energies of wild-type Ssh10b and its variants versus temperature: wild-type Ssh10b (*solid line*), P18A (*dashed line*), P62A (*dotted line*), and P18AP62A (*dashed dotted line*)

the configurational hindrance of the pyrrolidine ring (Suzuki et al. 1987; Matthews et al. 1987; Suzuki 1989). Therefore, proline residues are thought to play an important role in maintaining protein stability. It has been estimated that the stability of the native form of a protein increases by about 2–4 kJ/mol when a proline residue is introduced into a protein chain at a location that does not alter the protein structure (Matthews et al. 1987; Allen et al. 1998; Nicholson et al. 1992).

In this work, a series of Pro→Ala variants was constructed to study the stability contribution of the four proline residues in the protein Ssh10b. Using chromatography experiments we found that there is a kinetic equilibrium between the *cis*- and *trans*- forms of Ssh10b in solution due to the presence of Pro^{62}, agreeing well with published data (Cui et al. 2003). The Pro→Ala replacements in these variants did not cause substantial variation in the global secondary and tertiary structure of the protein, as judged from far- and near-UV CD measurements (Fig. 2).

However, the four single-site mutants in this study showed differences in stability. Unfolding curves of P6A, P8A and the Ssh10b wild-type were almost superimposable in both urea-induced and heat-induced experiments, suggesting that the Pro^6 and Pro^8 make little contribution to the stability of Ssh10b. We concluded that, in the folded state, these two residues may be very flexible, agreeing well with results from a previous report showing that no electron density was observed for the first eight amino

acids in the crystal structure of Ssh10b (Wardleworth et al. 2002).

Stability of the other two single-site mutants, P18A and P62A, decreased greatly relative to the Ssh10b wild-type. An interesting phenomenon was observed: urea-induced unfolding experiments at 298 K showed that P18A was more stable than P62A, while heat-induced unfolding experiments showed that P62A was slightly more stable than P18A. This phenomenon is consistent with the prediction of our unfolding model that the contribution of a proline residue to protein stability is connected with the thermodynamic equilibrium between the two isomers induced by the *cis–trans* isomerization of the peptide bond between the proline residue and its preceding residue both in unfolded and folded states.

According to the unfolding model described in "Materials and methods", relative to the unfolding free energy of P18AP62A, the increased unfolding free energy of protein P62A results from the contribution of the $Ala^{18}\rightarrow Pro^{18}$ replacement, which can be divided into two components: (1) a favorable contribution associated with lower configurational entropy of the proline residues in the unfolded state that can be represented as $\Delta\Delta G_{conf} = -T\Delta S$; and (2) an unfavorable contribution associated with the isomerization of peptide bonds Lys^{17}-Pro^{18} in the unfolded state that can be represented as $\Delta\Delta G_{18U} = -2RT \ln (1 + K_U(P18))$, where $K_U(P18)$ can be calculated through Eq. 16.

Relative to the unfolding free energy of P18AP62A, the increased unfolding free energy of protein P18A results from the contribution of the $Ala^{62}\rightarrow Pro^{62}$ replacement. Due to the presence of peptide bonds Leu^{61}-Pro^{62} isomerization in the native P18A, this contribution can be divided into three components: (1) a favorable contribution associated with lower configurational entropy of the proline residues in the unfolded state that can be represented as $\Delta\Delta G_{conf} = -T\Delta S$; (2) an unfavorable contribution associated with peptide bonds Leu^{61}-Pro^{62} isomerization in the unfolded state that can be represented as $\Delta\Delta G_{62U} = -2RT \ln (1 + K_U(P62))$, where $K_U(P62)$ can be calculated through Eq. 16; and (3) a favorable contribution associated with peptide bonds Leu^{61}-Pro^{62} isomerization in the native state that can be represented as $\Delta\Delta G_{62N} = RT \ln (1 + K_N(P62))$, where $K_N(P62)$ can be calculated through Eq. 16.

The difference in the unfolding free energy between P62A and P18A can be represented as $\Delta\Delta G_{diff} = \Delta\Delta G_{62N} + \Delta\Delta G_{62U} - \Delta\Delta G_{18U}$. Generally, $\Delta\Delta G_{62N}$ is associated with the ratio of *cis:trans* in peptide bonds Leu^{61}-Pro^{62} in the native state, and is temperature-dependent; $\Delta\Delta G_{62U}$ and $\Delta\Delta G_{18U}$ are associated with the ratio of *cis:trans* in peptide bonds Leu^{61}-Pro^{62} and Lys^{17}-Pro^{18} in the unfolded state, and are dependent on both primary sequence and temperature. As the *cis*-form of Leu^{61}-Pro^{62} dominates in native state and the values of $\Delta\Delta G_{62U}$ and $\Delta\Delta G_{18U}$ are similar at lower temperatures, $\Delta\Delta G_{diff}$ is mainly determined by $\Delta\Delta G_{62N}$. For example, the obtained values of these three sections at 298 K were: $\Delta\Delta G_{62N} =$ 2.9 kJ/mol, $\Delta\Delta G_{62U} = -2.1$ kJ/mol, $\Delta\Delta G_{18U} = -1.9$ kJ/mol, so the difference in the unfolding free energy between P18A and P62A was 2.7 kJ/mol, agreeing well with the difference of 3.3 kJ/mol obtained from urea-induced unfolding experiments. At higher temperatures, due to the overwhelming prevalence of the *trans*-form of Leu^{61}-Pro^{62} in native state, the value of $\Delta\Delta G_{62N}$ tends to zero; therefore the $\Delta\Delta G_{diff}$ is mainly determined by the slight difference between $\Delta\Delta G_{62U}$ and $\Delta\Delta G_{18U.}$ For example, the obtained values of these three section at 348 K were: $\Delta\Delta G_{62N} =$ 0.2 kJ/mol, $\Delta\Delta G_{62U} = -7.1$ kJ/mol, $\Delta\Delta G_{18U} = -6.2$ kJ/mol, so the difference in the unfolding free energy between P62A and P18A was −0.7 kJ/mol, agreeing well with the facts that in the heat-induced unfolding experiment P62A was slightly more stable than P18A within the melting region (about 335–360 K).

These arguments form the basis for explaining the interesting phenomenon described above. Therefore, we can conclude that proline residues play an important role in maintaining protein stability, but the contribution of a specific proline residue to protein stability is not only associated with its lower configurational entropy in the unfolded states but also associated with the thermodynamic equilibrium between *cis*- and *trans*-isomers both in the unfolded and folded states.

Acknowledgments This work was partially supported by grants from the Natural Science Foundation of China (No. 30870475 and No. 30670420) and the Program for Changjiang Scholars and Innovative Research Team in University.

References

Agashe VR, Udgaonkar JB (1995) Thermodynamics of denaturation of barstar: evidence for cold denaturation and evaluation of the interaction with guanidine hydrochloride. Biochemistry 34:3286–3299

Allen MJ, Countinho PM, Ford CF (1998) Stabilization of *Aspergillus awamori* glucoamylase by proline substitution and combining stabilizing mutations. Protein Eng 11:783–788

Chen BL, Schellman JA (1989) Low-temperature unfolding of a mutant of phage T4 lysozyme. 1. Equilibrium studies. Biochemistry 28:685–691

Cheng HN, Bovey FA (1977) *Cis-trans* equilibrium and kinetic studies of acetyl-L-proline and glycyl-L-proline. Biopolymers 16:1465–1472

Cui Q, Tong Y, Xue H, Huang L, Feng Y, Wang J (2003) Two conformations of Archaeal Ssh10b. J Biol Chem 278:51015–51022

Frare E, de Laureto PP, Scaramella E, Tonello F, Marin O, Deana R, Fontana A (2005) Chemical synthesis of the RGD-protein decorsin: Pro→Ala replacement reduces protein thermostability. Protein Eng Des Sel 18:487–495

Freire E (1995) Thermal denaturation methods in the study of protein folding. Methods Enzymol 259:144–168

Gåseidnes S, Synstad B, Jia X, Kjellesvik H, Vriend G, Eijsink VG (2003) Stabilization of a chitinase from *Serratia marcescens* by Gly→Ala and Xxx→Pro mutations. Protein Eng 16:841–846

Goihberg E, Dym O, Tel-Or S, Levin I, Peretz M, Burstein Y (2007) A single proline substitution is critical for the thermostabilization of *Clostridium beijerinckii* alcohol dehydrogenase. Proteins 66:196–204

Grathwohl C, Wüthrich K (1981) NMR studies of the rates of proline *cis-trans* isomerization in oligopeptides. Biopolymers 20:2623–2633

Hardy F, Veriend G, Veltman OR, van der Vinne B, Venema G, Eijsink VG (1993) Stabilization of *Bacillus stearotheromphilus* neutral protease by introduction of prolines. FEBS Lett 317:89–92

Kamal JK, Nazeerunnisa M, Behere DV (2002) Thermal unfolding of soybean peroxidase. Appropriate high denaturant concentrations induce cooperativity allowing the correct measurement of thermodynamic parameters. J Biol Chem 277:40717–40721

Li Y, Reilly PJ, Ford C (1997) Effect of introducing proline residues on the stability of *Aspergillus awamori*. Protein Eng 10:1199–1204

Mao YJ, Sheng XR, Pan XM (2007) The effects of NaCl concentration and pH on the stability of hyperthermophilic protein Ssh10b. BMC Biochem 8:28

Matthews BW, Nicholson H, Becktel WJ (1987) Enhanced protein thermostability from site-directed mutations that decrease the entropy of unfolding. Proc Natl Acad Sci USA 84:6663–6667

Némethy G, Leach SJ, Scheraga HA (1966) The influence of amino acid side chains on the free energy of helix-coil transitions. J Phys Chem 70:998–1004

Nicholson H, Tronrud DE, Becktel WJ, Matthews BW (1992) Analysis of the effectiveness of proline substitutions and glycine replacements in increasing the stability of phage T4 lysozyme. Biopolymers 32:1431–1441

Sakaguchi M, Matsuzaki M, Niimiya K, Seino J, Sugahara Y, Kawakita M (2007) Role of proline residues in conferring thermostability on aqualysin I. J Biochem 142:213–220

Santoro MM, Bolen DW (1988) Unfolding free energy changes determined by the linear extrapolation method. 1. Unfolding of phenylmethanesulphonyl alpha-chymotrypsin using different denaturants. Biochemistry 27:8063–8068

Schellman JA (1987) The thermodynamic stability of proteins. Annu Rev Biophys Chem 16:115–137

Sriprapundh D, Vieille C, Zeikus JG (2000) Molecular determinants of xylose isomerase thermal stability and activity: analysis of thermozymes by site-directed mutagenesis. Protein Eng 13:259–265

Suzuki Y (1989) A general principle of increasing protein thermostability. Proc Jpn Acad B Phys Biol Sci 65:146–148

Suzuki Y, Oishi Y, Nakano H, Nagayama T (1987) A strong correlation between the increase in number of proline residues and the rise in thermostability of five Bacillus oligo-1, 6-glucosidase. Appl Microbiol Biotechnol 26:546–551

Wardleworth BN, Russell RJ, Bell SD, Taylor GL, White MF (2002) Structure of Alba: an archaeal chromatin protein modulated by acetylation. EMBO J 21:4654–4662

Watanabe K, Masuda T, Ohashi H, Mihara H, Suzuki Y (1994) Multiple proline substitutions cumulatively thermostabilize *Bacillus cereus* ATCC7064 oligo-1, 6-glucosidase. Eur J Biochem 226:277–283

Xu S, Qin S, Pan XM (2004) Thermal and conformational stability of Ssh10b protein from archaeon *Sulfolobus shibatae*. Biochem J 382:433–440

Xue H, Guo R, Wen Y, Liu D, Huang L (2000) An abundant DNA binding protein from the hyperthermophilic archaeon *Sulfolobus shibatae* affects DNA supercoiling in a temperature-dependent fashion. J Bacteriol 182:3929–3933